

Plasmon-Mediated Organic Photoelectrochemistry Applied to Amination Reactions

Buravets, Vladislav; Gorin, Oleg; Burtsev, Vasilii; Zabelina, Anna; Zabelin, Denis; Kosina, Jiri; Maixner, Jaroslav; Svorcik, Vaclav; Kolganov, Alexander A.; Pidko, Evgeny A.

DOI

[10.1002/cplu.202400020](https://doi.org/10.1002/cplu.202400020)

Publication date

2024

Document Version

Final published version

Published in

ChemPlusChem

Citation (APA)

Buravets, V., Gorin, O., Burtsev, V., Zabelina, A., Zabelin, D., Kosina, J., Maixner, J., Svorcik, V., Kolganov, A. A., Pidko, E. A., & Lyutakov, O. (2024). Plasmon-Mediated Organic Photoelectrochemistry Applied to Amination Reactions. *ChemPlusChem*, 89(8), Article e202400020. <https://doi.org/10.1002/cplu.202400020>

Important note

To cite this publication, please use the final published version (if applicable).
Please check the document version above.

Copyright

Other than for strictly personal use, it is not permitted to download, forward or distribute the text or part of it, without the consent of the author(s) and/or copyright holder(s), unless the work is under an open content license such as Creative Commons.

Takedown policy

Please contact us and provide details if you believe this document breaches copyrights.
We will remove access to the work immediately and investigate your claim.

Plasmon-Mediated Organic Photoelectrochemistry Applied to Amination Reactions

Vladislav Buravets,^[a] Oleg Gorin,^[a] Vasilii Burtsev,^[a] Anna Zabelina,^[a] Denis Zabelin,^[a] Jiri Kosina,^[b] Jaroslav Maixner,^[b] Vaclav Svorcik,^[a] Alexander A. Kolganov,^[c] Evgeny A. Pidko,^[c] and Oleksi Lyutakov*^[a]

Organic electrochemistry is currently experiencing an era of renaissance, which is closely related to the possibility of carrying out organic transformations under mild conditions, with high selectivity, high yields, and without the use of toxic solvents. Combination of organic electrochemistry with alternative approaches, such as photo-chemistry was found to have great potential due to induced synergy effects. In this work, we propose for the first time utilization of plasmon triggering of enhanced and regio-controlled organic chemical transformation performed in photoelectrochemical regime. The advantages of the proposed route is demonstrated in the model amination

reaction with formation of C–N bond between pyrazole and substituted benzene derivatives. Amination was performed in photo-electrochemical mode on the surface of plasmon active Au@Pt electrode with attention focused on the impact of plasmon triggering on the reaction efficiency and regio-selectivity. The ability to enhance the reaction rate significantly and to tune products regio-selectivity is demonstrated. We also performed density functional theory calculations to inquire about the reaction mechanism and potentially explain the plasmon contribution to electrochemical reaction rate and regioselectivity.

Introduction

Although the organic electrochemistry, i.e. the ability to perform the chemical transformation of organic molecules on the surface of the electrode(s) under the application of external bias, was discovered more than 100 years ago, this synthetic strategy experiences a rebirth nowadays.^[1–4] The renaissance of the organic electrochemistry is boosted through the synergy brought by its integration with additional and alternative reaction optimization and selectivity controlling strategies, such as transition-metal-catalysis, dual electrocatalysis, and cascade catalysis.^[5–9] A particularly attractive approach towards milder reaction conditions and improved selectivity control is the synergistic use of photo- and electro-organocatalysis for targeted organic synthesis.^[10–13]

One of the common techniques in organic photo-electrochemistry is the use of dye molecules as the additives to the reaction mixture.^[14–16] These molecules are excited by photons and then they interact with charge (electrons or holes) injected from an external bias source. However, utilization of light should not be restricted to the utilization of dye excitation, dissolved in the organic mixture.^[17] Intensive research in the field of energy storage revealed that in the processes such as water splitting, CO₂ reduction and nitrogen activation, the photons can be used for additional enhancement of the catalytic activity of the electrode(s).^[18–25] In these regards, the utilization of combined photo-electrochemical approach is especially effective with additional sub-diffraction light focusing, which can be achieved on plasmon active nanostructures.^[26–28] Such nanostructures can convert the photons in plasmons with gigantic concentration of light energy (initially smeared in the space) and in a such way works as a sub-diffraction lens.^[29–31] If the layer of catalytically-active material is placed in the closed space of such plasmonic field, its catalytic activity can be enhanced significantly, due to easier interface charge transfer, overall increase of free charge numbers and various other phenomena.^[32–34] Such approach is widely used in the field of “relevant” chemical transformation triggering (such as mentioned above water splitting,^[35] CO₂ reduction,^[33,36] nitrogen activation^[37]) but, to the best of our knowledge, was not reported in the area of organic electrocatalysis.^[38,39]

Plasmon-assisted chemistry has also been reported in the field of organic chemical transformations. In this case, the plasmon can accelerate or induces the reaction of organic substrates through the injection of a hot electron(s) on lower unoccupied orbital(s) of organic substrate or inner-molecular electron excitation.^[40] As an example, the formation of hydro-

[a] V. Buravets, O. Gorin, V. Burtsev, A. Zabelina, D. Zabelin, V. Svorcik, O. Lyutakov
Department of Solid State Engineering, University of Chemistry and Technology, Technicka 5, 166 28 Prague, Czech Republic
E-mail: lyutakoo@vscht.cz

[b] J. Kosina, J. Maixner
Central Laboratories, University of Chemistry and Technology, Technicka 5, 166 28 Prague, Czech Republic

[c] A. A. Kolganov, E. A. Pidko
Inorganic Systems Engineering, Department of Chemical Engineering, Faculty of Applied Sciences, Delft University of Technology, Van der Maasweg 9, Delft 2629 HZ, Netherlands

Supporting information for this article is available on the WWW under <https://doi.org/10.1002/cplu.202400020>

© 2024 The Authors. ChemPlusChem published by Wiley-VCH GmbH. This is an open access article under the terms of the Creative Commons Attribution Non-Commercial License, which permits use, distribution and reproduction in any medium, provided the original work is properly cited and is not used for commercial purposes.

generation of nitro compounds, degradation of organic pollutants and dyes, or Suzuki coupling can be mentioned.^[41–43] Most of these reactions were performed with the utilization of a localized plasmon; however, traveling surface plasmon-polariton can also be used for plasmon-mediated chemistry.^[44]

In this work we propose combination of organo-electrochemistry and plasmon assisted photo-chemistry as a promising approach to C–H amination – a practically relevant and challenging organic chemistry transformation.^[45] We use the bimetallic electrode (Au@Pt) combining the catalytic (Pt) and plasmon (Au) properties for the reaction proceeding in the photo-electrochemical mode. The main focus of our research is on unravelling the role of the plasmon in the reaction yield and regio-selectivity. The experimental observations are clarified by supporting atomistic density functional theory (DFT) calculations.

Results and Discussion

Preparation of Plasmon-Active Electrode

The preparation of plasmon active electrode is schematically depicted in Figure 1A. Briefly, excimer laser was used for the polymer surface patterning with subsequent deposition of two metals – plasmon active Au layer (25 nm thick) and catalytically active Pt layer (5–7 nm thick). Created structure combines the plasmonic properties, i.e. excitation of so-called surface plasmon polariton (SPP) wave under the light illumination at corresponding wavelength and the redox activity (ensured by the presence of catalytically active Pt layer). The electrode morphology, measured by scanning electron microscopy (SEM) and atomic force microscopy (AFM) techniques is shown in Figure 1B. As can be seen, samples possess grating like pattern, which is required for the excitation of SPP wave.^[46] Subsequent UV-Vis measurements reveal the position of SPP absorption band with the maximum located at 702 nm for Au@Pt grating (Figure 1C). As is evident, the deposition of Pt layer (on the surface of the plasmon active Au grating) conserved the presence of the plasmon absorption band, but led to its red shift and widening. Additional characterization of Au@Pt

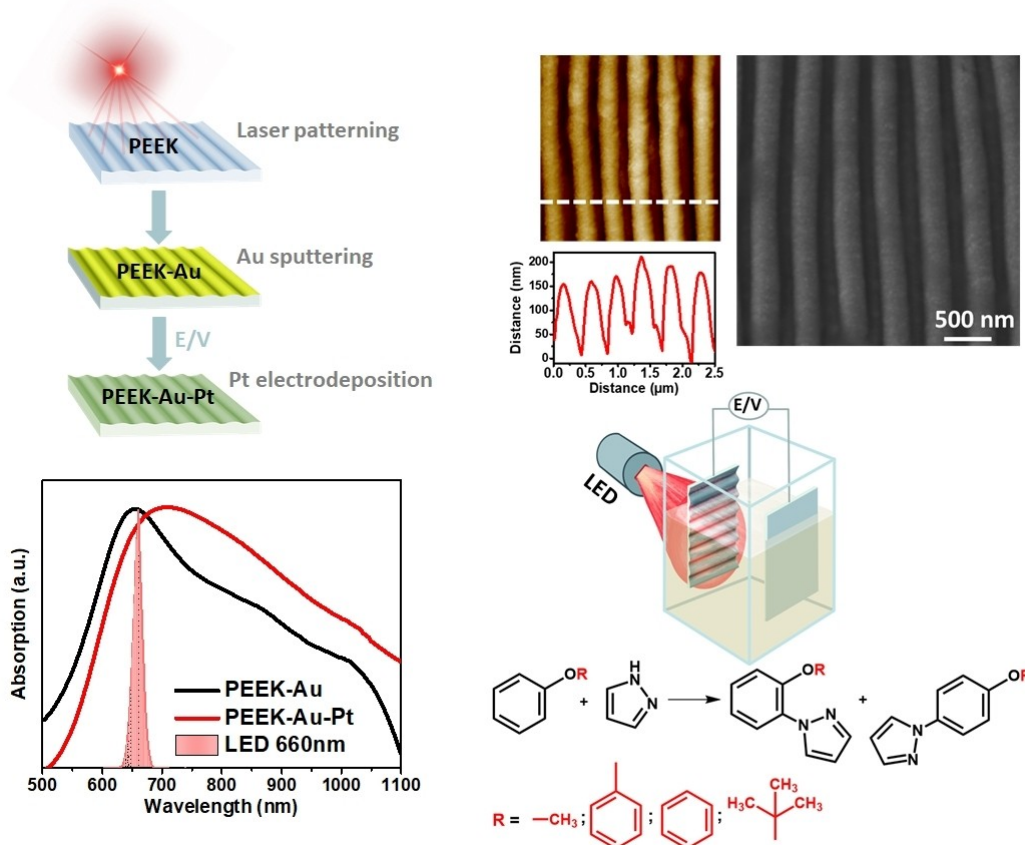


Figure 1. (A) – Schematic representation of Au@Pt photo-electrode preparation: creation of grating-like polymer template, Au sputtering, and Pt electrochemical deposition; (B) – Au@Pt grating surface morphology measured by AFM (including surface profile and SEM); (C) – UV-Vis absorption spectra of pristine Au grating and Au@Pt grating (emission spectrum of used LED is also presented); (D) – schematic representation of experimental set-up and C–H amination with the formation of ortho- and para-regioisomers.

grating (Figure S1–S3 and related discussion) is given in SI. Subsequent photo-electrochemical experiments (Figure 1D) were performed in photo-electrochemical mode using light emitting diode (LED) source with wavelength corresponding to SPP excitation on Au@Pt grating surface. Relevant C–H amination reaction (Figure 1D) was chosen as a model one to estimate the plasmon triggering impact on the reaction proceeding. In particular, we used the reaction between pyrazole and several substituted anisole(s), with main attention focused on “model” pyrazole – anisole reaction (for estimation of plasmon-induced changes in the reaction rate and yield), while the different benzene derivatives were used to check the plasmon-induced changes in the reaction regio-selectivity.

Plasmon Assisted Photo-Electrochemical C–H Amination – Model Case

First, to reveal potentials required for amination (pyrazole and anisole model case) linear sweep voltammetry (LSV) measurements were performed (Figure 2A). LSV curves were recorded in

dark and under plasmon triggering illumination. In both cases the current onset was observed at ~ 2 V, independently on illumination mode. In turn, LSV curve shift induced by electrode surface illumination reveals current enhancement under plasmon triggering. Based on the LSV measurements, a potential of 3.6 V was chosen as a reaction driving force for time resolved analysis, since at this potential the significant current density was observed (at least for presented model “anisole-pyrazole” case). Resulted chronoamperometric curves, obtained at this potential in dark and under plasmon triggering illumination, are presented in Figure 2B. As is evident, plasmon triggering results in greater current density, which could be expected from previously measured LSV curves. Additionally, we also observed enhancement of current density after reaction start in photo-electrochemical mode, which can be attributed to a plasmon-heating effect (based on the observed time-scale). Then a gradual decrease of the current as a function of reaction time was observed, which can be assigned to the depletion of the reactants concentration in the electrolyte.

Subsequent analysis of the reaction products, performed with utilization of gas chromatography-mass spectrometry (GS-

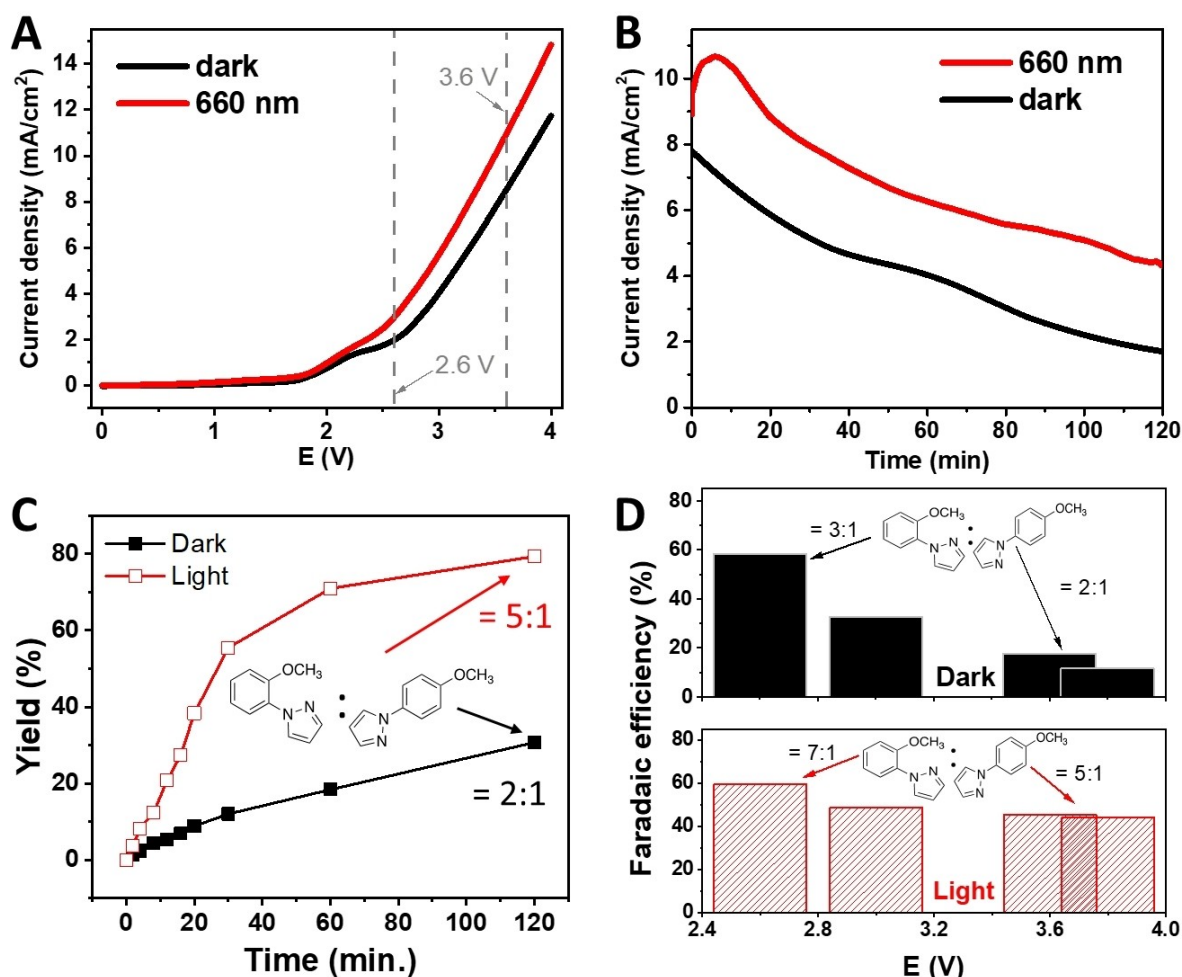


Figure 2. (A) – LSV curves, measured during C–H amination (pyrazole and anisole model case) proceeding on Au@Pt grating electrode surface in dark or under illumination (i.e. with plasmon assistance); (B) – chronoamperometric curves measured during amination proceeding in dark and light under 3.6 V vs RHE potential; (C) – time-resolved yields and regioisomers ratio of methoxyphenyl-1H-pyrazole obtained in the dark or under plasmon-assisted C–H amination; (D) – Faradaic efficiency of C–H amination and produced regioisomers ratio as a function of used potential with or without plasmon triggering.

MS) approach (Figure S4), indicates that in both, dark and light cases the creation of ortho and para regioisomers (1-(2-Methoxyphenyl)-1H-pyrazole and 1-(4-Methoxyphenyl)-1H-pyrazole) is observed. Time-resolved yields and regioisomers ratio of methoxyphenyl-1H-pyrazole obtained in the dark or under plasmon-assisted C–H amination are presented in Figure 2C. As is evident, the plasmon triggering significantly accelerates the reaction rate and after 2 hours of reaction process the yield under illumination achieves almost 80% (for both regioisomers), compared to 27% in the dark case (since the gold is completely covered by the Pt film, the dark case can be considered as a “traditional” Pt electrode, applied in the electrochemical mode). Moreover, plasmon triggering also results in significant changes of ortho: para (o:p) regioisomers ratio – we observed the 5:1 ratio in photoelectrochemical mode vs 2:1 in dark one. Similar prevalence of the traditionally anomalous (from steric reasons)^[47–49] ortho isomer was previously observed for photo-electrochemical amination with utilization of semiconductor-based photoelectrode.^[50] In our case we also observed pronounced shift of reaction selectivity towards ortho isomer with utilization of additional, plasmon assisted energy input into the reaction mixture.

Taking into account some discrepancy in the plasmon induced increase of current density (see Figures 2A, B) and regioisomers yield (Figure 2C) we also paid attention to one of the crucial parameter in electrocatalysis - Faradaic efficiency

(FE).^[51] In particular, part of the charge carriers delivered to the electrochemical cell can be used for amination, while rest can be spent in parasitic reactions (e.g. methanol oxidation). In these regards it is important to estimate the FE as a function of both, applied potential and plasmon triggering. The calculated values of FE are presented in Figure 2D. As is evident, in “dark” conditions apparent decrease of the FE with increasing potential is observed, indicating that the alternative reactions become dominant process at higher potential. Conversely, in the case of plasmon assistance the reaction is more selective, the FE also decreases at higher potentials, but only moderately, exceeding 40% for “higher” potentials.

In the next step, we performed an additional investigation of C–H amination with pyrazole and several alternative organic substrates (substituted benzene rings). Particularly diphenyl ether, benzyl phenyl ether, tert-butoxybenzene were used. In this case, our main attention was focused on the impact of plasmon triggering on the reaction regio-selectivity. The obtained results are presented in Figure 3 (Figures S4–S7 show the GS-MS spectra; the positions of the regioisomers were determined using a standard). As is evident, in several cases we observed the formation of just one ortho-isomer in the dark (designated as “T”, while the absence of the other regio-isomer is designated as “N” in Figure 3),. Plasmon triggering resulted in significant amount of reaction products and formation of both ortho and para regio-isomers. In particular, we observed almost

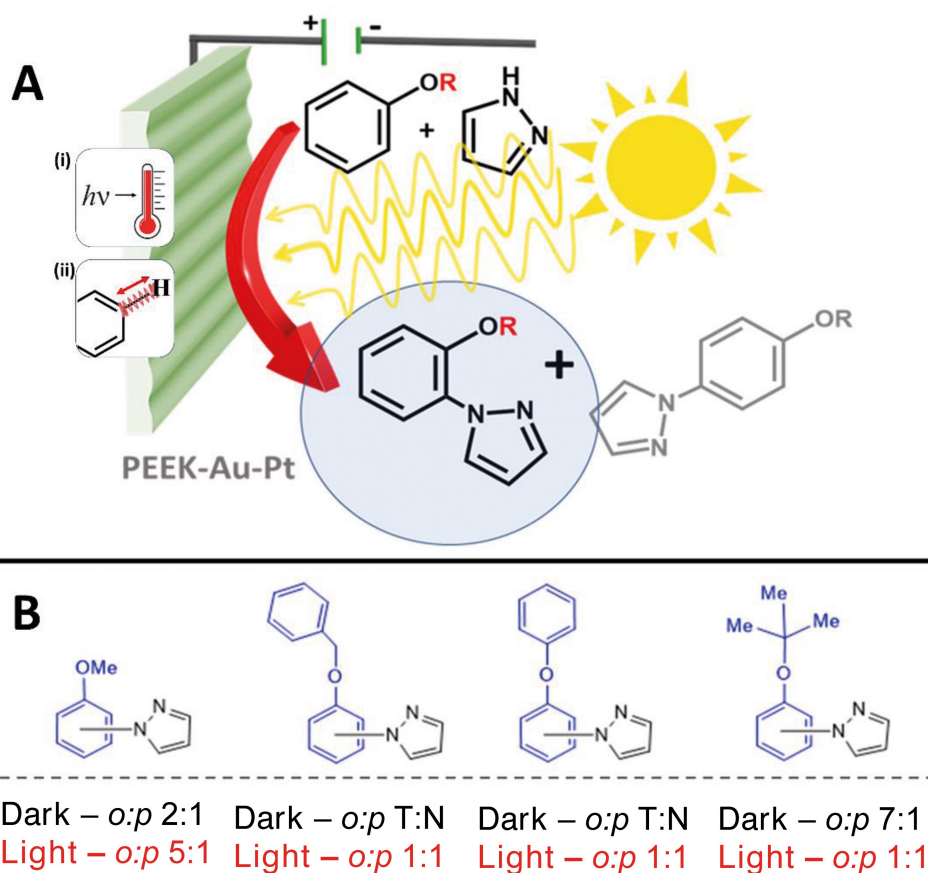


Figure 3. (A) – Schematic representation of C–H amination (pyrazole and benzene derivatives) performed in plasmon-assisted photoelectrochemical mode and (B) – ratio of ortho:para regioisomers, obtained with (Light) or without (Dark) plasmon triggering.

equivalent formation of regio-isomers in the case of diphenyl ether, tert-butoxybenzene, and benzyl phenyl ether (para isomers were not observed under dark conditions, without plasmon triggering), which are traditionally considered as a 'hard' substrate for C–H amination in ortho position. Thus, plasmon triggering not only increases the efficiency of the reaction with the utilisation of various benzene derivatives, but also allows tuning of the reaction regio-selectivity.

Alternative Reactions and Potential Mechanism

In view of the unusual impact of plasmon triggering, on reaction yield, regio-isomers ratio and FE, we attempted to explain the reaction mechanism and the potential impact of plasmon triggering by implementation of the electrochemical measurements in three electrode setup and quantum mechanics calculations. First, the linear sweep voltammetry curves suggest that anisole is the first to be involved in the reaction (pyrazole and anisole were measured separately; see Figure S8). Thus, in the subsequent density function theory (DFT) calculations, we proceed with anisole (as well as other benzene derivatives) as the model substrate.

The results of DFT calculations are summarized in Figure 4 and Figures S9–S13. First, we exclude the recently proposed mechanism postulating the formation of radical-cation from

anisole, because it would thermodynamically and kinetically favour the production of the para-isomers (Figure S9), which is in contrast to the experimental data. As an alternative reaction path, we propose the elimination of an H atom from the anisole assisted by the Pt(111) surface (Figure S10).^[52] We can thus hypothesize that this step is the rate-determining one as it features the breaking of the anisole aromatic system. The subsequent step infers the direct insertion of a pyrazole molecule on the carbon that lost the H atom. Therefore, we only focused on the H-atom abstraction by Pt(111) as this step should determine the observed experimentally regio-selectivity.

Since the H atom abstraction by Pt should be a function of the orientation of the organic molecules on the electrode surface, we considered two possible adsorption configurations of anisole (and other benzene derivatives) on the bridge30 (b30)^[53] site of the Pt (111) surface as schematically presented in Figure 4A. The results show that the adsorption mode with methoxy group in non-apical substitution (denoted as 'asymmetric' adsorption) is slightly more energetically favourable than apical substitution (denoted as 'symmetric' adsorption).^[53]

The influence of the anisole functionalization and its adsorption orientation on the Pt surface is summarized in Figure 4B. The formation of an ortho isomer is more thermodynamically favourable in the case of asymmetric orientation for all benzene derivatives. These calculation results perfectly correlate with the data in Figure 4A (which confirms the

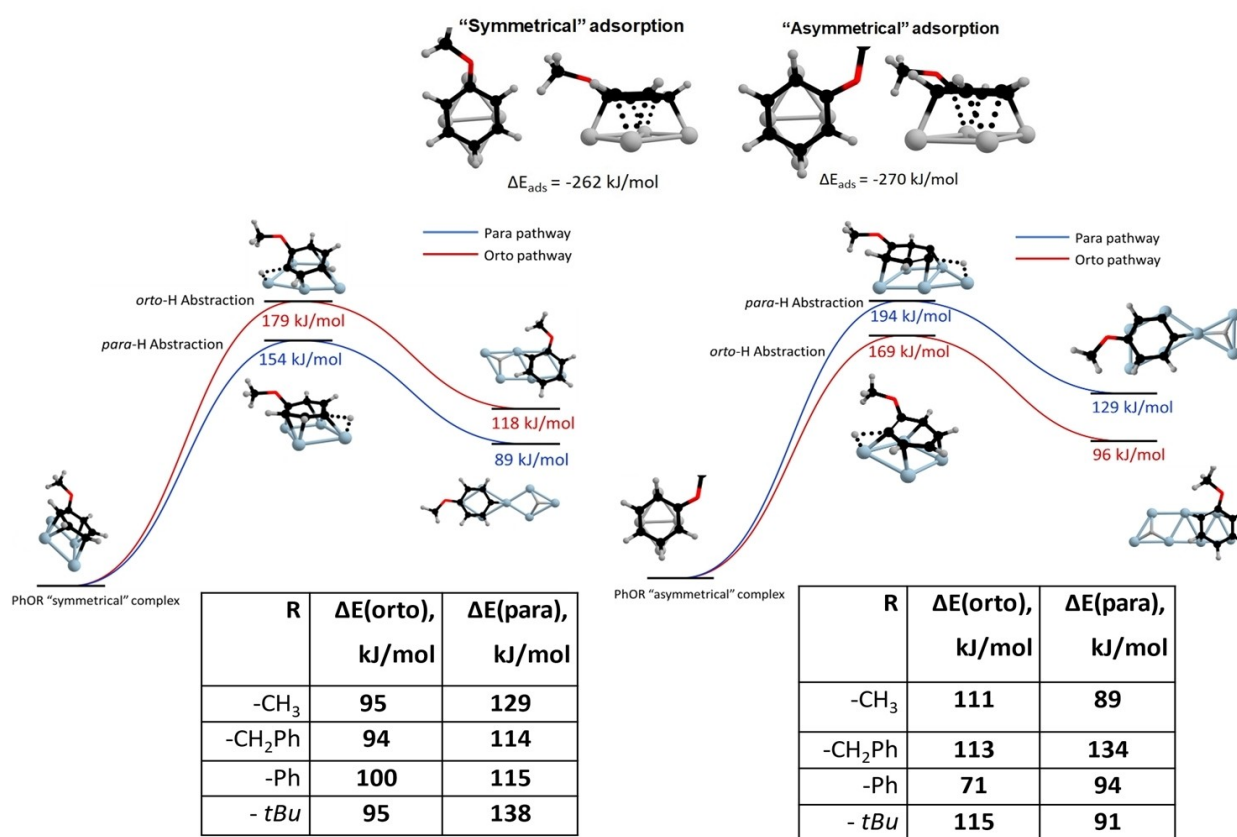


Figure 4. (A) – Two possible modes of anisole adsorption on Pt surface; (B) – predicted reaction pathways and corresponding ΔE of H-elimination of the reaction starting from "symmetrical" and (C) "asymmetrical" benzene derivative adsorption complexes.

dominant asymmetric surface adsorption), as well as with the experimental results in Figure 3B (dark case). In particular, the lower energy required for the elimination of an H atom led to the subsequent addition of pyrazole to the ortho position, when the reaction is performed in the dark, which is in agreement with the experimental results showing the dominant production of the ortho regioisomers. We could assume both radical-cation and heterogeneous mechanisms could co-exist in the system and that the plasmon heating effect increases the local temperature of the Pt surface, thus making the high-barrier surface reaction, which initially involves the breaking of the anisole aromatic system, more accessible. Alternatively, a significant local value of the electric component of the plasmon evanescent wave can also lead to the polarisation of chemical bonds in the adsorbed organic molecule and in this way lead to the more simple elimination of H atom from both the ortho and para positions in the benzene ring.

At this stage, it is difficult to accurately assess the mechanism of plasmonic influence. However, taking into account the present results, it can be argued that the mechanism differs from some traditionally considered one in the field of plasmon-assisted photochemistry (i.e. from hot electron injection or inner electron excitation). In particular, our results show that the transfer of hot electrons or holes, as well as the excitation of the internal electrons in organic molecules, probably do not occur in the case of plasmon-assisted organic electrochemistry (at least in the case presented here). The observed increase in reaction kinetics and the shift in selectivity should be more likely correlated with the induced polarisation of the organic molecule in a "strong" plasmonic field and/or with local plasmonic heating. In other words, we assume that both cation-radical and heterogeneous mechanisms can co-exist in the system and that the plasmon heating effect increases the local temperature of the Pt surface, thus making the high-barrier surface reaction, which initially involves the breaking of the anisole aromatic system, more accessible. Alternatively, a significant local value of the electric component of the plasmon evanescent wave can also lead to the polarization of chemical bonds in the adsorbed organic molecule and in this way lead to a more simple elimination of H atom from both ortho and para positions in the benzene ring. Both effects (plasmon heating and polarization of chemical bonds) were introduced into Figure 3A.

Conclusions

In this work, the advantage of plasmon triggering of C–H amination, performed in the photo-electrochemical mode, was demonstrated. Reaction was performed on the surface of a plasmon- and catalytically-active Au@Pt electrode. Plasmon contribution in the reaction rate and regio-selectivity (formation of ortho- or para- isomers) was investigated. It was demonstrated that plasmon triggering significantly enhances the C–H amination rate, which was observed for anisole and several benzene derivatives. Plasmon triggering also allows to compensate for the significant decrease of the Faradaic efficiency,

observed when C–H amination is performed at higher applied potentials. In addition, plasmon enhancement has a strong impact on the reaction regio-selectivity. We also performed density functional theory calculations, which indicate that C–H amination with a high probability proceeds through elimination of the H atom from the benzene ring with subsequent addition of the pyrazole molecule. In this sense, the impact of plasmon triggering can be attributed to a local heating or additional polarisation of molecular bond(s) in anisole molecules.

Thus, our work shows for the first time that the combination of organic electrocatalysis with plasmon-assisted chemistry results in reaction acceleration, increases the energy efficiency (especially at high potentials/currents), and can tune the reaction (regio-)selectivity. We believe that these benefits can be further extended to wide range of organic electrochemical reactions.

Experimental Section

Materials

Amorphous polyether ether ketone (PEEK) sheets with thickness of 25 μm were purchased from the Goodfellow Ltd. Methanol (99.93%) was purchased from Lachner. Sulfuric acid (96%) was obtained from Penta. Potassium tetrachloroplatinate(II) (K_2PtCl_4 , 99%), pyrazole (synthesis quality), lithium perchlorate (LiClO_4 , 98%) were purchased from Sigma-Aldrich. Gold target (99.99% purity) was purchased from Safina a.s. Pyrazole, anisole, benzyl phenyl ether, benzyl phenyl ether, and phenyl t-butyl ether were purchased from Sigma-Aldrich.

Samples Preparation and Characterization

PEEK thin films were patterned using the KrF excimer laser with 248 nm emission wavelength (COMPexPro 50 F, Coherent, Inc., USA). Incident angle of laser beam was 45° in regards to PEEK surface normal, laser fluency was 6.5 mJ/cm^2 , number of counts – 4000. Grating-like pattern was created on $1 \times 0.7 \text{ cm}^2$ sample area using the additionally introduced aperture.

Deposition of thin gold films by plasma sputtering was performed using Quorum Q150R. Electrochemical deposition of Pt was achieved with utilization of PalmSens4 potentiostat combined with PSTrace software. Pt deposition was performed from 0.5 M H_2SO_4 with 10 mM K_2PtCl_4 water solution, by running one cycle of cycling voltammetry (CV) in ranges between 0.82 V to -0.18 V vs RHE at 50 mV/s scan rate,

For samples illumination and plasmon excitation the light emitting diode with 660 nm central wavelength and 40 mW/cm^2 irradiance on the sample surface (ThorLabs) was used.

SEM images were obtained using LYRA3 GMU (Tescan). Surface morphology analysis was performed on AFM by Bruker Corp., model Dimension ICON. UV-Vis spectra were recorded by Lambda 25 (PerkinElmer). XRD patterns were obtained using PANanalytical X Pert PRO (Malvern PANanalytical). X-ray photoelectron spectroscopy (XPS) was measured on ESCAProbeP (Omicron Nanotechnology Ltd). Electrochemical measurements were done using PalmSens4 potentiostat.

Plasmon-assisted C–H Electrochemical Amination

Reaction was performed in the two-electrode setup with engineered plasmon-active electrode as the working electrode (WE) and platinum foil as a counter electrode (CE). Electrolyte for the reaction setup was composed out of methanol as a solvent with addition of 0.1 M LiClO₄. The concentration of the added reagents was 133 mM of pyrazole and 66 mM of anisole. For proper illumination of the WE, UV-Vis cuvette was employed as an electrochemical cell with 3D-printed cap to provide fixation and connection to the WE and CE. Light irradiance on a first glass surface was adjusted to 100 mW/cm²

Products Characterization

For the qualitative analysis GC-MS was performed on Agilent 7200 Q-TOF, column DB1 5 m×0.32 mm film 0.25 μm+restrictor 1 m×0.15 mm, with following parameters set: He to 1 ml/min 40 °C (4 min) – 10 °C/min – 300 °C (5 min), inlet 250 °C, split 20. In MS measurements the ionization energy was set to 70 eV, with 5 scans/s for the range of 20–600 ms. Standards for product analysis (1-(2-Methoxyphenyl)-1H-pyrazole and 1-(4-Methoxyphenyl)-1H-pyrazole) were purchased from Biosynth. The structures of the rest of chemicals was determined using separately prepared p-regioisomers (produced by Enamine). The enantiomers ratio(s) was determined after reaction proceeding using GC peaks ratio and separately created calibration curves (obtained by several subsequent dilution of reaction mixture and GC measurement).

Supporting Information

The authors have cited additional references within the Supporting Information.^[54–65]

Acknowledgements

This work was supported by the GACR under project 23-08509S. The use of Dutch National supercomputer facilities was sponsored by NWO Domain Science. Open Access publishing facilitated by Vysoka skola chemicko-technologicka v Praze, as part of the Wiley - CzechELIB agreement.

Conflict of Interests

The authors declare no conflict of interest.

Data Availability Statement

The data that support the findings of this study are available from the corresponding author upon reasonable request.

Keywords: plasmon-assisted chemistry · organic electrocatalysis · C–H activation · amination · regio-selectivity

[1] H. Kolbe, *J. Prakt. Chem.* **1847**, *41*, 137–139.

- [2] M. Faraday, *Ann. Phys.* **1834**, *109*, 481–520.
[3] C. Zhu, N. W. J. Ang, T. H. Meyer, Y. Qiu, L. Ackermann, *ACS Cent. Sci.* **2021**, *7*, 415–431.
[4] M. Yan, Y. Kawamata, P. S. Baran, *Chem. Rev.* **2017**, *117*, 13230–13319.
[5] K. Mahanty, S. Kumar Saha, A. Halder, S. D. Sarkar, *Chem. Commun.* **2023**, *59*, 4467–4470.
[6] X. Hu, I. Cheng-Sánchez, S. Cuesta-Galisteo, C. Nevado, *J. Am. Chem. Soc.* **2023**, *145*, 6270–6279.
[7] C. Ma, P. Fang, Z.-R. Liu, S.-S. Xu, K. Xu, X. Cheng, A. Lei, H.-C. Xu, C. Zeng, T.-S. Mei, *Sci. Bull.* **2021**, *66*, 2412–2429.
[8] N. E. S. Tay, D. Lehnher, T. Rovis, *Chem. Rev.* **2022**, *122*, 2487–2649.
[9] Y. Yu, P. Guo, J.-S. Zhong, Y. Yuan, K.-Y. Ye, *Org. Chem. Front.* **2020**, *7*, 131–135.
[10] H. Kim, H. Kim, T. H. Lambert, S. Lin, *J. Am. Chem. Soc.* **2020**, *142*, 2087–2092.
[11] Y. Yuan, J. Yang, J. Zhang, *Chem. Sci.* **2023**, *14*, 705–710.
[12] T. Shen, Y.-L. Li, K.-Y. Ye, T. H. Lambert, *Nature* **2023**, *614*, 275–280.
[13] J. Liu, C. Xia, S. Zaman, Y. Su, L. Tan, S. Chen, *J. Mater. Chem. A* **2023**, *11*, 16918–16932.
[14] W. Zhang, K. L. Carpenter, S. Lin, *Angew. Chem.* **2020**, *132*, 417–425.
[15] H. Yan, Z. Hou, H. Xu, *Angew. Chem. Int. Ed.* **2019**, *58*, 4592–4595.
[16] H. Huang, Z. M. Strater, M. Rauch, J. Shee, T. J. Sisto, C. Nuckolls, T. H. Lambert, *Angew. Chem. Int. Ed.* **2019**, *58*, 13318–13322.
[17] L. Zhang, L. Liardet, J. Luo, D. Ren, M. Grätzel, X. Hu, *Nat. Catal.* **2019**, *2*, 366–373.
[18] P. Subramanyam, B. Meena, V. Biju, H. Misawa, S. Challapalli, *J. Photochem. Photobiol. C* **2022**, *51*, 100472.
[19] A. Zabelina, J. Dedek, O. Guselnikova, D. Zabelin, A. Trelin, E. Miliutina, Z. Kolska, J. Siegel, V. Svorcik, J. Vana, O. Lyutakov, *ACS Catal.* **2023**, *13*, 3830–3840.
[20] S. Wang, Y. Zhang, Y. Zheng, Y. Xu, G. Yang, S. Zhong, Y. Zhao, S. Bai, *Small* **2023**, *19*, 2204774.
[21] A. Zabelina, E. Miliutina, D. Zabelin, V. Burtsev, V. Buravets, R. Elashnikov, V. Neubertova, M. Štastrný, D. Popelková, J. Lancok, S. Chertopalov, M. Paidar, A. Trelin, A. Michalčová, V. Švorčík, O. Lyutakov, *J. Chem. Eng.* **2023**, *454*, 140441.
[22] H. Wang, C. Cheng, K. Du, Z. Xu, E. Zhao, N. Lan, P.-F. Yin, T. Ling, *Chem. Eur. J.* **2023**, *29*, e202300204.
[23] M. Duca, M. T. M. Koper, in *Surface and Interface Science* (Ed.: K. Wandelt), Wiley, **2020**, pp. 773–890.
[24] Z. Zhang, C. Zhang, H. Zheng, H. Xu, *Acc. Chem. Res.* **2019**, *52*, 2506–2515.
[25] E. Kazuma, Y. Kim, *Angew. Chem. Int. Ed.* **2019**, *58*, 4800–4808.
[26] L. Mascaretti, A. Dutta, Š. Kment, V. M. Shalaev, A. Boltasseva, R. Zbořil, A. Naldoni, *Adv. Mater.* **2019**, *31*, 1805513.
[27] O. Guselnikova, P. Postnikov, M. M. Chehimi, Y. Kalachyova, V. Svorcik, O. Lyutakov, *Langmuir* **2019**, *35*, 2023–2032.
[28] Q. Wang, K. Domen, *Chem. Rev.* **2020**, *120*, 919–985.
[29] N. P. de Leon, B. J. Shields, C. L. Yu, D. E. Englund, A. V. Akimov, M. D. Lukin, H. Park, *Phys. Rev. Lett.* **2012**, *108*, 226803.
[30] L. Wang, M. Hasanzadeh Kafshgari, M. Meunier, *Adv. Funct. Mater.* **2020**, *30*, 2005400.
[31] S. Li, P. Miao, Y. Zhang, J. Wu, B. Zhang, Y. Du, X. Han, J. Sun, P. Xu, *Adv. Mater.* **2021**, *33*, 2000086.
[32] O. Guselnikova, A. Olshtrem, Y. Kalachyova, I. Panov, P. Postnikov, V. Svorcik, O. Lyutakov, *J. Phys. Chem. C* **2018**, *122*, 26613–26622.
[33] M. Tahir, M. Siraj, B. Tahir, M. Umer, H. Alias, N. Othman, *Appl. Surf. Sci.* **2020**, *503*, 144344.
[34] S. Lincic, S. Chavez, R. Elias, *Nat. Mater.* **2021**, *20*, 916–924.
[35] D. B. Ingram, S. Lincic, *J. Am. Chem. Soc.* **2011**, *133*, 5202–5205.
[36] J. Liu, C. Xia, S. Zaman, Y. Su, L. Tan, S. Chen, *J. Mater. Chem. A* **2023**, *11*, 16918–16932.
[37] M. Ali, F. Zhou, K. Chen, C. Kotzur, C. Xiao, L. Bourgeois, X. Zhang, D. R. MacFarlane, *Nat. Commun.* **2016**, *7*, 11335.
[38] S. Chen, W.-H. Li, W. Jiang, J. Yang, J. Zhu, L. Wang, H. Ou, Z. Zhuang, M. Chen, X. Sun, D. Wang, Y. Li, *Angew. Chem. Int. Ed.* **2022**, *61*, e202114450.
[39] S. Chen, Z. Zhang, W. Jiang, S. Zhang, J. Zhu, L. Wang, H. Ou, S. Zaman, L. Tan, P. Zhu, E. Zhang, P. Jiang, Y. Su, D. Wang, Y. Li, *J. Am. Chem. Soc.* **2022**, *144*, 12807–12815.
[40] Z. Zhang, C. Zhang, H. Zheng, H. Xu, *Acc. Chem. Res.* **2019**, *52*, 2506–2515.
[41] F. Chen, Q. Yang, C. Niu, X. Li, C. Zhang, G. Zeng, *RSC Adv.* **2015**, *5*, 63152–63164.
[42] B. Mondal, P. S. Mukherjee, *J. Am. Chem. Soc.* **2018**, *140*, 12592–12601.

- [43] F. Wang, C. Li, H. Chen, R. Jiang, L.-D. Sun, Q. Li, J. Wang, J. C. Yu, C.-H. Yan, *J. Am. Chem. Soc.* **2013**, *135*, 5588–5601.
- [44] H. L. Luk, J. Feist, J. J. Toppari, G. Groenhof, *J. Chem. Theory Comput.* **2017**, *13*, 4324–4335.
- [45] A. Ricci, *Amino Group Chemistry: From Synthesis to the Life Sciences*, Wiley-VCH, Weinheim, **2008**.
- [46] Y. Kalachyova, O. Lyutakov, P. Slepicka, R. Elashnikov, V. Svorcik, *Nanoscale Res. Lett.* **2014**, *9*, 591.
- [47] V. Sukowski, M. van Borselen, S. Mathew, M. Á. Fernández-Ibáñez, *Angew. Chem. Int. Ed.* **2022**, *61*, e202201750.
- [48] N. A. Romero, K. A. Margrey, N. E. Tay, D. A. Nicewicz, *Science* **2015**, *349*, 1326–1330.
- [49] K. A. Margrey, J. B. McManus, S. Bonazzi, F. Zecri, D. A. Nicewicz, *J. Am. Chem. Soc.* **2017**, *139*, 11288–11299.
- [50] L. Niu, H. Yi, S. Wang, T. Liu, J. Liu, A. Lei, *Nat. Commun.* **2017**, *8*, 14226.
- [51] P. A. Kempler, A. C. Nielander, *Nat. Commun.* **2023**, *14*, 1158.
- [52] R. Réocreux, C. A. Ould Hamou, C. Michel, J. B. Giorgi, P. Sautet, *ACS Catal.* **2016**, *6*, 8166–8178.
- [53] N. Bonalumi, A. Vargas, D. Ferri, A. Baiker, *J. Phys. Chem. B* **2006**, *110*, 9956–9965.
- [54] A. Bard, *Standard Potentials in Aqueous Solution*, Routledge, **2017**.
- [55] O. Diaz-Morales, T. J. P. Hersbach, C. Badan, A. C. Garcia, M. T. M. Koper, *Faraday Discuss.* **2018**, *210*, 301–315.
- [56] F. Neese, *WIREs Comput. Mol. Sci.* **2022**, *12*, e1606.
- [57] A. V. Marenich, C. J. Cramer, D. G. Truhlar, *J. Phys. Chem. B* **2009**, *113*, 6378–6396.
- [58] G. Henkelman, B. P. Uberuaga, H. Jónsson, *J. Chem. Phys.* **2000**, *113*, 9901–9904.
- [59] T. D. Kühne, M. Iannuzzi, M. Del Ben, V. V. Rybkin, P. Seewald, F. Stein, T. Laino, R. Z. Khaliullin, O. Schütt, F. Schiffmann, D. Golze, J. Wilhelm, S. Chulkov, M. H. Bani-Hashemian, V. Weber, U. Borstnik, M. TAILLEFUMIER, A. S. Jakobovits, A. Lazzaro, H. Pabst, T. Müller, R. Schade, M. Guidon, S. Andermatt, N. Holmberg, G. K. Schenter, A. Hehn, A. Bussy, F. Belleflamme, G. Tabacchi, A. Glöß, M. Lass, I. Bethune, C. J. Mundy, C. Plessl, M. Watkins, J. VandeVondele, M. Krack, J. Hutter, *J. Chem. Phys.* **2020**, *152*, 194103.
- [60] S. Grimme, S. Ehrlich, L. Goerigk, *J. Comput. Chem.* **2011**, *32*, 1456–1465.
- [61] S. Goedecker, M. Teter, J. Hutter, *Phys. Rev. B* **1996**, *54*, 1703–1710.
- [62] J. VandeVondele, J. Hutter, *J. Chem. Phys.* **2007**, *127*, 114105.
- [63] B. G. Lippert, J. H. Parrinello, M. Parrinello, *Mol. Phys.* **1997**, *92*, 477–488.
- [64] R. Kronberg, K. Laasonen, *ACS Catal.* **2021**, *11*, 8062–8078.
- [65] H. B. Michaelson, *J. Appl. Phys.* **2008**, *48*, 4729–4733.

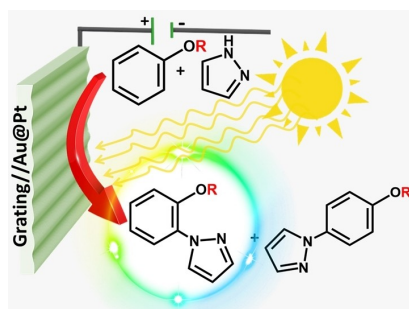
Manuscript received: January 9, 2024

Revised manuscript received: April 8, 2024

Version of record online: ■■, ■■

RESEARCH ARTICLE

Plasmon-mediated organic electrochemistry: C–H amination reaction yield and regio-selectivity can be sufficiently enhanced/tuned with utilization of plasmon assistance and bimetallic (catalytic- and plasmon active) electrode.



V. Buravets, O. Gorin, V. Burtsev, A. Zabelina, D. Zabelin, J. Kosina, J. Maixner, V. Svorcik, A. A. Kolganov, E. A. Pidko, O. Lyutakov*

1 – 9

Plasmon-Mediated Organic Photoelectrochemistry Applied to Amination Reactions

